AIP | Journal of Applied Physics

Bond length variation in In0.25Ga0.75As/InP epitaxial layers thicker than the critical thickness

M. Tormen, D. De Salvador, M. Natali, A. Drigo, F. Romanato et al.

Citation: J. Appl. Phys. 86, 2533 (1999); doi: 10.1063/1.371088
View online: http://dx.doi.org/10.1063/1.371088
View Table of Contents: http://jap.aip.org/resource/1/JAPIAU/v86/i5
Published by the American Institute of Physics.

Bond length variation in $In_{0.25}Ga_{0.75}As/InP$ epitaxial layers thicker than the critical thickness

M. Tormen, D. De Salvador, M. Natali, and A. Drigo[a)]
Dipartimento di Fisica ''G. Galilei'' via Marzolo 8, Istituto Nazionale Fisica della Materia (INFM), I-35131 Padova, Italy

F. Romanato
TASC-INFM at Elettra Synchrotron, SS.14 Km 163.5, I-34012 Basovizza, Trieste, Italy

G. Rossetto
Instituto Chimica Tecn. Inorganiche Materiali Avanzati (ICTIMA-CNR), Corso Stati Uniti 4, I-35020 Padova, Italy

F. Boscherini
Laboratori Nazionali di Frascati, INFN, P.O. Box 13, I-00044 Frascati, Italy

S. Mobilio
Laboratori Nazionali di Frascati, INFN, P.O. Box 13, I-00044 Frascati, and Dipartimento di Fisica, Universita Roma Tre, Via della Vasca Navale 84, 00146 Roma, Italy

(Received 4 January 1999; accepted for publication 20 May 1999)

We address the issue of the local structure in an epitaxial semiconductor thin film undergoing strain relaxation due to extended defects when the critical thickness for their introduction is exceeded. The nearest neighbor environment is probed by x-ray absorption fine structure spectroscopy. The particular system studied is a set of $In_{0.25}Ga_{0.75}As$ films grown on InP(001) of increasing thickness; the thicknesses were chosen so as to obtain a varying degree of relaxation, ranging from pseudomorphic growth to completely relaxed state. The samples have been thoroughly characterized with complementary structural techniques and the residual strain is measured by x-ray diffraction. We find that the Ga–As bond length exhibits a linear decrease with decreasing residual strain. By comparing these results with previous studies on bond lengths in pseudomorphic $In_xGa_{1-x}As$ films as a function of concentration we conclude that the bond lengths have an identical behavior as a function of the mean residual strain independently from its elastic or plastic origin. This result is reproduced by an analytical model based on the transfer of the mean macroscopic deformation at a local level. The broadening of the bond length distribution induced by extended defects is also discussed, concluding that it is not experimentally dectable. © *1999 American Institute of Physics.* [S0021-8979(99)01717-X]

I. INTRODUCTION

It is well known that the strain can affect the optical (band gap, transition rate)[1] and electronic properties (carrier mean free path and mobility, band alignment) of semiconductor heterostructures as well as their thermal stability.[2,3] Recent theoretical work has shown that these effects cannot be accurately reproduced using an approximate atomic distribution—the most used being that resulting from the application of the strain field to the virtual crystal approximation (VCA).[4,5] On the contrary, knowledge of the strain effects on each type of atomic bond represents the basic information for the optoelectronic structure determination of strained semiconductor alloys.

In epitaxial heterostructures three different effects contribute to the bond deformation: (1) the coexistence in the alloy of bonds of different nature (alloying disorder), (2) the epitaxial constraint imposed by the substrate (epitaxial strain), and (3) the strain field induced by the presence of extended defects (plastic strain).

The effect of alloying has been studied in the past, both theoretically and experimentally. X-ray absorption fine structure (XAFS) investigations in bulk semiconductor pseudobinary alloys such as $In_xGa_{1-x}As$[6] or $Cd_xMn_{1-x}Te$[7] have shown that the nearest neighbor interatomic distances exhibit a bimodal distribution with a weak compositional dependence. These results have definitively rejected the VCA hypothesis of floppy bonds in favor of valence force field models that successfully account for the bimodal atomic distribution considering both bond stretching and bond bending forces.[8,9]

The effect on the local structure of the biaxial strain in pseudomorphic layers has been addressed more recently. In particular XAFS studies of pseudomorphic $In_xGa_{1-x}As$ grown on GaAs[10] or on InP(001)[11] have been reported. By measuring As–In and Ga–As bond lengths in a number of samples as a function of indium concentration, x, (and thus of the strain) it was possible to demonstrate that bond length variation is proportional to biaxial strain,[11] a result that also

a)Electronic mail: drigo@padova.infm.it

TABLE I. Structural parameters of the investigated samples (25 at.% In atomic fraction, misfit 1.95×10^{-2}) Columns 1-5: sample code, film thickness t, strain along [110], $[1\bar{1}0]$, and average biaxial strain $\epsilon_{\parallel}$ (HRXRD). Columns 6 and 7 report the difference between GaAs bond length in strained and unstrained InGaAs defined by $\delta r^{st}=r_{GaAs}-r^{*}_{GaAs}$ ($r^{*}_{GaAs}=2.448+0.035*x$ is the Ga–As bond length in bulk), and the first shell Debye–Waller parameter.

Code	t (nm)	$\epsilon_{[110]}$ (%)	$\epsilon_{[1\bar{1}0]}$ (%)	$\epsilon_{\parallel}$ (%)	δr^{st} (Å) ±0.003	σ^2 10^{-3} Å^2 ±0.4
A	26	1.91	1.95	1.93	0.017	3.2
B	150	0.90	1.68	1.29	0.010	2.6
C	600	0.13	0.72	0.42	0.006	3.5
D	2400	0.08	0.2	0.14	0.001	3.1

can be reproduced by random-cluster calculations[12] or by a simple analytical model.[11]

The effects of plastic defects on the local structure strain are less known. Misfit dislocations and other extended defects are introduced in epitaxial strained heterostructures in order to release the elastic strain energy when the layer thickness exceeds a critical value. The initial misfit is then slowly relaxed by the average plastic strain field increasing the defect density as a function of the thickness. In the present work we report an investigation of the effects at local level of the strain relaxation process induced by plastic defects. We have monitored the bond length changes obtained by varying the thickness of a series of $In_{0.25}Ga_{0.75}As$ epilayers grown on (001) InP substrates. The same issue has been already addressed in previous articles[13,14] where the bond length deformations were plotted and discussed as a function of film thickness. However, the choice of this functional dependence reduces the generality of those results because the strain released by defect formation depends on the specific kind of alloy, substrate and growth conditions, and on the nature of the defects. In our work we have chosen to relate the bond length directly to the mean residual strain measured by high resolution x-ray diffraction (HRXRD). Comparing the present results with previously published data[11] on $In_xGa_{1-x}As$/InP pseudomorphic epilayers, we show that the bond length variation introduced by the average strain does not depend on whether the origin of the strain is plastic or elastic.

It is well known that the plastic strain field exhibits a signficant nonuniformity due to the large strain field close to the defects. The effects of a distribution of strain in the sample volume on the bond length have thus been estimated for the analyzed samples and discussed.

II. EXPERIMENTAL AND XAFS DATA ANALYSIS

We have investigated four $In_{0.25}Ga_{0.75}As$ epitaxial films with thickness ranging between 25 and 2400 nm which will be denoted as samples A, B, C, and D, ordered according to their thickness (see Table I). Samples were deposited by metal-organic vapor phase epitaxy on InP [001] substrates at a temperature of 650 °C.

The samples have been precharacterized by HRXRD and Rutherford backscattering spectroscopy (RBS), in order to obtain the strain and the composition, by atomic force microscopy (AFM) and transmission electron microscopy (TEM) to characterize the surface morphology and the plastic defects, while the local structure has been studied by XAFS.

AFM micrographs have been collected with a Park Scientific Instruments microscope in the ''contact mode'' using Ultralever™ (Ultralever is a trademark of Park Scientific Instruments) tips in order to minimize the tip-surface convolution.

TEM investigations to evaluate the layer microstructure, misfit, and threading dislocation densities have been performed with a JEOL 2000 FX microscope operated at 200 kV. (001) plan and (110) oriented cross sections were prepared by a conventional mechanochemical thinning procedure followed by room temperature Ar ion milling.

HRXRD measurements were performed with a Philips MRD high resolution x-ray diffractometer using Cu $K\alpha$ radiation monochromatized by a Ge220 Bartels monochromator and a Ge crystal analyzer in front of the detector. The strain in the InGaAs layers has been determined following standard procedures[15] collecting at the four azimuths along the $\langle110\rangle$ in plane directions $\omega-2\theta$ scans of the 004 and 444 reflections. An upper limit to the strain distribution in the layer was determined by measuring the layer peak full width at half maximum (FWHM) of the 004 rocking curves.

RBS-channeling measurements were performed using a 2 MeV ^{4}He beam delivered by the AN-2000 Van der Graaff accelerator of the National Laboratories of Legnaro (Italy).

XAFS measurements were performed at the European Synchrotron Radiation Facility (ESRF) in Grenoble (France) at the GILDA beamline, using a dynamical sagitally focusing Si(311) monochromator;[16] higher harmonics were rejected by a pair of grazing incidence, Pd coated, mirrors. The spot size was approximately 1×2 mm^2 and the photon flux approximately 5×10^{10} photons per second. Fluorescence detection was performed with a seven element hyperpure Ge detector; the shaping time on the amplifiers was 0.25 μs and the total count rate on each detector element was limited to 30 000 counts/s to avoid nonlinearity problems. The measurements were performed at 77 K in order to reduce the thermal vibration. In order to have a pure signal of the first coordination shell and then a better estimate of the Ga–As distance, the XAFS data were collected at the Ga K edge instead of the As K edge in order to avoid the chemical mixing of the nearest neighbor shell present around As atoms.

In our samples the high quality crystalline substrate affected the absorption spectra with spurious peaks due to the occurrence of Bragg reflections. These reflections alter the absorption signal in two ways: either reaching directly one or more detector elements and saturating them, or by modulating the fluorescence intensity with the excitation of x-ray standing waves (the latter effect, as opposed to the former, is present in the signal from all detector signals at the same time). The seven element detector allows to overcome the detector saturation problem by averaging the seven detector

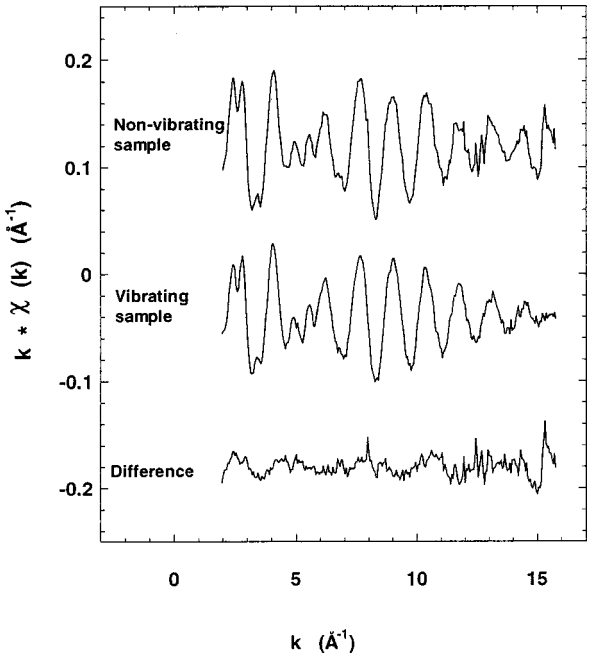

FIG. 1. Comparison of XAFS spectra obtained in the case of fixed and vibrating sample ($In_{0.53}Ga_{0.47}As$ measured at the As *K* edge).

signals, in order to improve the signal to noise ratio after the exclusion of the saturated channels.

To reduce the excitation of standing waves we mounted the samples on a homebuilt vibrating sample holder (VISAH) which continuously changes the Bragg condition during data collection, completely smoothing out the spurious peaks. The VISAH consists of a cantilever made of Cu–Be (this material was chosen for its good thermal conductivity and elasticity), 10 cm long, fixed inside the experimental vacuum chamber at one edge to a liquid nitrogen cryostat and terminating at the opposite end in a plate hosting a variable number of samples (4–7). An external electromagnet acting on an iron disk fixed under the plate drives the vibration of the cantilever. A capacitive sensor provides the feedback to maintain the vibration in its first resonance mode (~ 70 Hz), whose amplitude can be controlled in the range of 0.1–2 mm; the corresponding maximum angular spread is of the order of 1 deg. The sample holder was oriented in such a way that the normal to the sample surface forms an angle of 20 deg with respect to the x-ray beam and an angle of 70 deg with respect to the beam polarization. The noise level in the absorption signal was of the order of $\sim 10^{-3}$ with 10 s integration time and was not affected by the sample vibration. Figure 1 shows the smoothing effect on the spurious signal features: notice especially the features above 12.5 $Å^{-1}$ disappearing when the sample vibrates.

XAFS spectra were collected in the 10 150–11 700 eV energy range. Data analysis was performed by the GNXAS package[17] which provides an *ab initio* modeling of XAFS signal. The GNXAS code allows a least square fitting procedure performed directly on the raw experimental data. The absorption background was evaluated and subtracted by fitting the pre-edge region with a linear function in the interval -200 to -50 eV below the edge (10 363 eV). The atomic

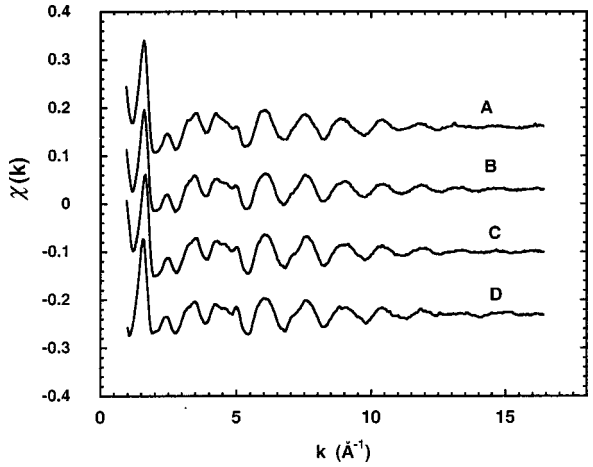

FIG. 2. XAFS spectra of samples **A**–**D** after background removal and normalization.

absorption was estimated by three cubic splines whose spline parameters have been optimized during the fitting process at the same time of the structural parameters. The raw, background-extracted XAFS oscillations for all samples, extending up to 17 $Å^{-1}$, are shown in Fig. 2 and the high quality is apparent. Above 5 $Å^{-1}$ the signal is dominated by a single frequency originating from the first shell.

In the present article the analysis of the local environment around Ga was limited to the first shell. Consequently, the experimental signal was fitted with only one single theoretical contribution due to four As nearest neighbors (NN) in the range of 3.0–16.0 $Å^{-1}$. Exceptionally, the spectrum relative to sample **D** was analyzed in the 3.0–12.0 $Å^{-1}$ interval due to the presence of some spurious features in the spectrum (the VISAH was accidentally not operational). To enhance the information relative to the first shell, with respect to the higher shells, a k^2 weighting was used. The set of fitting parameters consisted in the Ga–As bond distance R, the Debye–Waller parameter σ^2, the binding energy E_0 of 1*s* electrons in Ga, and the many-body amplitude reduction factor S_0^2. The error estimate was obtained following the procedures described in Ref. 17 for the confidence interval of 1 s.d.

III. RESULTS

The main important structural parameters of the analyzed epitaxial layers have been reported in Table I. Indium atomic fraction, film thickness and residual strain have been determined after a cross check of the RBS channeling and HRXRD analysis.

The surface morphology was investigated by AFM. Whereas for the pseudomorphic sample **A** the surface was atomically flat, the surface of the relaxed layers was characterized by arrays of surface grooves (with average distance of the order of 1 μm, and depth of the order of 10% of the layer thickness) and ridges with heights of the order of some nm corresponding to the intersection of the microcracks with the free surface.

The defect structure was determined by TEM and cathode luminescence (CL).[9] In the relaxed samples we have

observed misfit dislocations at the interface, twins, stacking-fault lamellae, and microcracks. The average distance between the microcracks (cracks were not observed on pseudomorphic sample **A**) was of the order of few μm. By HRXRD we found that the strain in the layers along the two $\langle 110 \rangle$ directions in the interface have a pronounced asymmetry. Such asymmetries are typical of the strain relaxation process in InGaAs/InP tensile layers.[18,19] The difference between the strains along the two directions is maximum for layers with partial strain relaxation, in our case for sample **B**, where $\epsilon_{[1\bar{1}0]} = 1.68\%$ and $\epsilon_{[110]} = 0.9\%$. In Table I we have reported the value of the strain parallel to surface averaged along the two in plane $\langle 110 \rangle$ directions.

The strain field generated by the large density of the different types of defect is not uniform. The extent of the strain distribution can be evaluated by high-resolution x-ray diffraction measuring the widths of the peak layer $\omega - 2\theta$ rocking curve. Actually also the finite thickness of the layer and composition fluctuations contribute to broaden the layer peak whose FWHM therefore gives only an upper limit to the strain distribution FWHM, i.e., $\mathrm{FWHM}_{\mathrm{strain}} < \mathrm{FWHM}_{\mathrm{layer\ peak}}/\tan$ (Bragg angle).

We investigated the strain nonuniformity in sample **B** for which the plastic strain-relaxation process is at an initial stage and in sample **D** where nearly all the strain was relaxed by defects. The layer peaks give an equivalent FWHM of the strain distribution which for sample **B** is 0.8% along [110] and 0.3% along $[1\bar{1}0]$ while for sample **D** is 0.4% along [110] and 0.36% along $[1\bar{1}0]$. However, a width of 0.07% may still derive from lateral composition fluctuations that we have estimated from RBS analysis to be within $\delta x < 1\%$. The contribution to the XRD peak broadening due to the finite layer thickness for the (004) reflection using Cu $K\alpha$ radiation is given by FWHM(arcsec) $= 18.66/\mathrm{L}(\mu\mathrm{m})$ and for the analyzed samples is still negligible leading to an equivalent strain broadening that in the worst case (sample **B**) is of 0.09%.

Table I reports the variation of the Ga–As bond lengths obtained by the XAFS analysis. Figure 3 shows the fit quality in k space for all samples together with the residual, i.e., the difference with respect to the experimental spectrum. It is clear that the main low frequency signal, due to the first shell, is very well fitted. The residual is due to the signal from the second and higher coordination shells and noise. In Fig. 4 the comparison between experiment and fit is performed in R space by showing the magnitude of the Fourier transform, performed in the range of 3.0–16.0 $\mathrm{\AA}^{-1}$. The overall factor S_0^2 and the Debye–Waller parameter σ^2 obtained in the analysis are, respectively, 0.95 ± 0.06 and $(3.1 \pm 0.4)10^{-3}$ Å. The procedures used in the present analysis are the same as those used for the analysis of the pseudomorphic samples[11] and of the InAs and GaAs model compounds. As a cross check of these results a second data analysis was done using the FEFF code, obtaining exactly the same bond length values, except for a rigid shift of 0.01 Å for all samples.

In order to demonstrate that the XAFS signals are sensitive to strain, Fig. 5 compares the first shell filtered signals of the pseudomorphic and more relaxed samples (**A** and **D**).

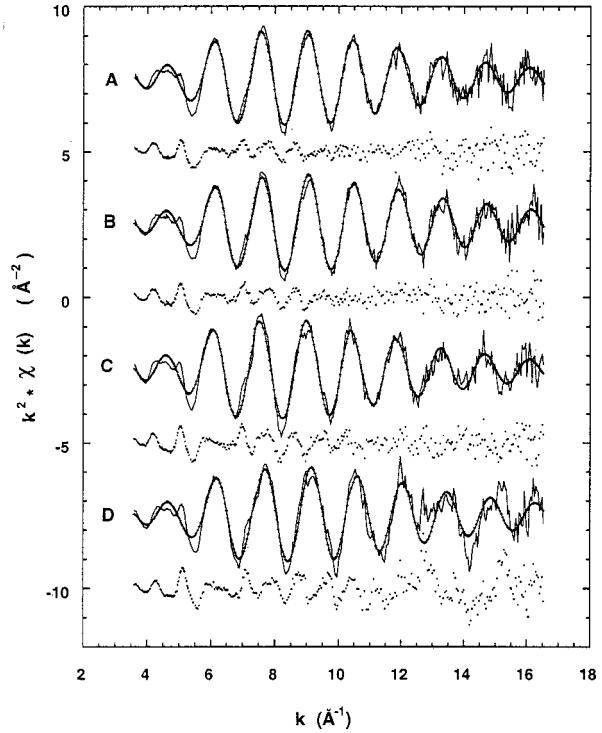

FIG. 3. Experimental $\chi(k)$ (multiplied by k^2 weight), and residuals. The features present in the residuals are clearly relative to higher coordination shells.

Filtered signals have been obtained by inverse Fourier transforms in the range of 1.2–3.0 Å.

To extract the contribution to the bond length variation due to the strain we have followed the analysis already proposed in Ref. 11. The variation of the Ga–As bond length with respect to the bond length in bulk GaAs, δr, has been decomposed in two contributions. The first one, δr^{al}, is the bond length variation due to the alloying. This is a strain independent effect that is present also in unstrained bulk material. We have estimated δr^{al} following the model proposed by Cai and Thorpe (CT)[9] that accounts precisely for the NN distances in InGaAs bulk alloys.[6] The second contribution,

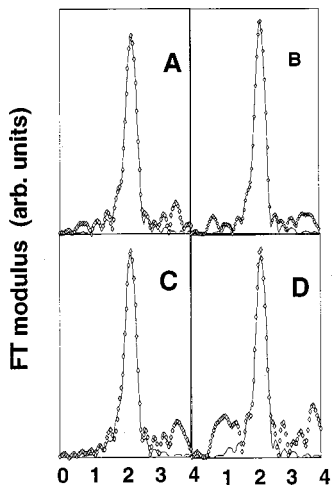

FIG. 4. Fourier transformed spectra (diamonds) and first shell fittings (continuous lines).

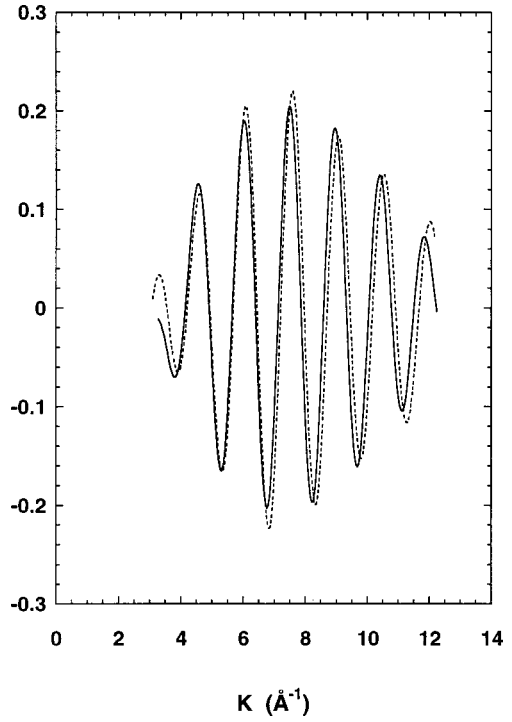

FIG. 5. Comparison between the first shell filtered signal for the most relaxed (dot line) and the pseudomorphic epilayers (continuous line).

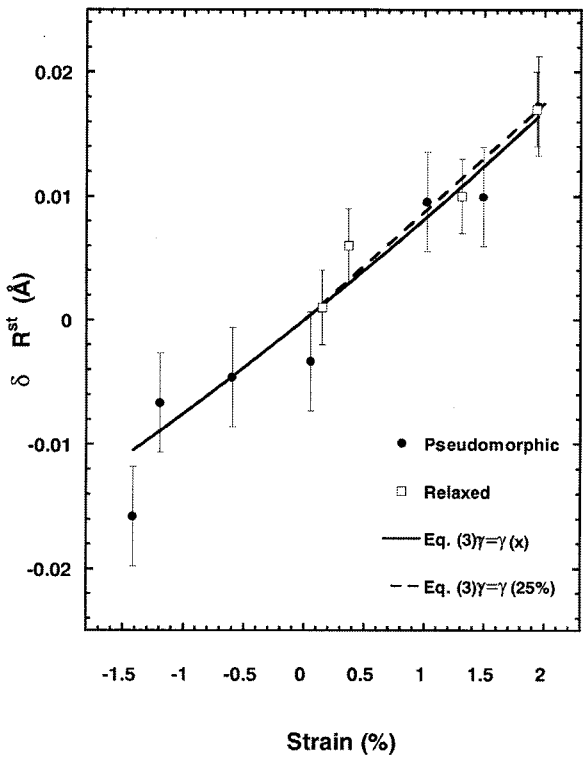

FIG. 6. Variation of Ga–As bond length with respect to the corresponding values in bulk $In_xGa_{1-x}As$ for pseudomorphic samples (full circles) and relaxed samples (squares).

δr^{st}, represents the effect of strain that includes the parts due to both epitaxial constraint and plastic defects.

The values of δr^{st} reported in Table I have been determined by subtracting to the XAFS measured δr the alloying contribution, δr^{al}. When plotted as a function of the average strain, the values of δr^{st} show a clear linear functional dependence (Fig. 6). Moreover the present data are well superimposed to the data relative to the pseudomorphic samples with different compositions reported in our previous work.[11]

IV. DISCUSSION

The bond length variation δr^{st} introduced by strain is reflected by the linear dependence shown in Fig. 6 and it can be predicted by a simple model. The basic assumption is the transferability of the macroscopic strain deformation down to a local scale. In other words, this model predicts that the bond vectors are deformed according to the macroscopic strain tensor $\bar{\bar{\epsilon}}$.

The outline of the derivation is the following:

In the virtual crystal approximation[4,5] for the zincblende structure there are four possible directions of the bond vectors $\mathbf{s}_1=a/4(1,1,1)$, $\mathbf{s}_2=a/4(-1,-1,1)$, $\mathbf{s}_3=a/4(-1,1,-1)$, and $\mathbf{s}_4=a/4(1,-1,-1)$, where a is the lattice parameter. In a real alloy the atoms are displaced from the virtual crystal sites by a vector $\mathbf{u}$ because of the alloying static disorder. The vector $\mathbf{u}$ is site-dependent, i.e., the deformation is different according to the nature of the bond (in the present case In–As and Ga–As) and to the nature of the surrounding atoms. The transferability of the macroscopic strain to the atomic scale can be written as

$$\delta r^{st}=|\mathbf{s}+\mathbf{u}+\bar{\bar{\epsilon}}(\mathbf{s}+\mathbf{u})|-|\mathbf{s}+\mathbf{u}|. \tag{1}$$

Equation (1) can be simplified taking into account that the strain tensor eigenvalues are small compared to unity. Rewriting the modulus as the square root of the square of the arguments Eq. (1) reads:

$$\delta r^{st}=\sqrt{(\mathbf{s}+\mathbf{u})^2+2(\mathbf{s}+\mathbf{u})\cdot\bar{\bar{\epsilon}}(\mathbf{s}+\mathbf{u})+[\bar{\bar{\epsilon}}(\mathbf{s}+\mathbf{u})]^2}-\sqrt{(\mathbf{s}+\mathbf{u})^2}. \tag{2}$$

For small value of the strain the term quadratic in strain under square root can be neglected with respect to the linear one; the zero order terms cancel out. The remaining first order term can be expressed as:

$$\delta r^{st}=\left(\frac{\mathbf{s}\cdot\bar{\bar{\epsilon}}\mathbf{s}+2\mathbf{s}\cdot\bar{\bar{\epsilon}}\mathbf{u}+\mathbf{u}\cdot\bar{\bar{\epsilon}}\mathbf{u}}{|\mathbf{s}+\mathbf{u}|}\right). \tag{3}$$

We can evaluate the order of magnitude of each term in this relation: the typical strain values in the investigated epitaxial films does not exceed 2%, the VCA vectors $\mathbf{s}$ have a modulus of about 2.4 Å and the vector $\mathbf{u}$ which describes the alloying distortion is of the order of 0.1 Å. From these orders of magnitude it follows that the first term in the brackets is some 10^{-2} Å, the second is some 10^{-3} Å, and the third is of the order of 10^{-4} Å. Neglecting the last two terms and introducing the strain tensor for a tetragonal distortion Eq. (3) becomes

$$\delta r^{st}=\frac{a(x)}{4\sqrt{3}}[2-\gamma(x)]\epsilon_{\|}, \tag{4}$$

where the constant γ is a combination of the elastic constant C_{11} and C_{12} of the material ($\gamma=2\times C_{12}/C_{11}$) and relates the

parallel and the perpendicular strain by the Poisson's equation $\epsilon_{\perp} = -\gamma\epsilon_{\parallel}$. Equation (4) is a linear relation between the bond stretching and the biaxial strain that depends on the indium atomic fraction only through the lattice parameter $a(x)$ and the constants $C_{11}(x)$ and $C_{12}(x)$. These functions of the compositions are evaluated, as usual, by a linear interpolation of the limit compound values. Equation (4) has been already presented in a more general version in our previous work[11] where the phenomenological force disorder parameter, ξ, which took into account the possible different elastic constant in the deformation of Ga–As and In–As bond lengths had been introduced. As we showed, the precision of XAFS is not sufficient to discriminate different values of the ξ parameter that, therefore, in the present work has been set equal to zero for simplicity. Use of this value, corresponding to the hypothesis of unique atomic forces, is furthermore justified in the present work because only Ga-As bond length values have been considered.

It must be observed that in the case of a tetragonal lattice distortion the stretching predicted by the Eq. (4) is the same for the four bonds $\mathbf{s_1}$, $\mathbf{s_2}$, $\mathbf{s_3}$, and $\mathbf{s_4}$, because they have the same projections (in modulus) on the principal strain axes. However, the present samples are not exactly tetragonally distorted. Because of the asymmetry in the strain release, the lattice undergoes an orthorhombic distortion. In this case the bond length offset δr^{st} is split in two values, one δr_{+}^{st} for bond vectors $\mathbf{s_1}$ and $\mathbf{s_2}$, the other δr_{-}^{st} for bond vectors $\mathbf{s_3}$ and $\mathbf{s_4}$, i.e.,

$$\delta r_{\pm}^{\mathrm{st}} = \frac{a}{4\sqrt{3}}(2-\gamma)\epsilon_{[1\pm10]} \pm \frac{a}{8\sqrt{3}}(2-\gamma)[\epsilon_{[110]} - \epsilon_{[1-10]}], \tag{5}$$

where $\epsilon_{[1\pm10]}$ are the parallel strains in the two $\langle 110\rangle$ directions. As the XAFS data collection were performed keeping the x-ray beam polarization near the normal to the sample (20° off), the different bond sets $\mathbf{s_i}$ have the same geometrical configuration with respect to the polarization providing, consequently, XAFS signals with the same statistical weight (within 10%). In particular, it results that the measured value of δr^{st} represents the average of the bond length variations due to the strain relaxation along both the $\langle 110\rangle$ in plane direction, i.e., $\delta r^{\mathrm{st}} = (\delta r_{+}^{\mathrm{st}} + \delta r_{-}^{\mathrm{st}})/2$, that therefore can still be obtained by the Eq. (5) and is exactly described by Eq. (4) where the parallel strain is defined as the average of the strain in the two directions.

In Fig. 6 the function described by Eq. (4) appears to perfectly interpolate all the available data points. This level of agreement was already shown for the pseudomorphic samples.[11] The new result of this work is that Eq. (4) is able to describe both the pseudomorphic samples, in which the strain is uniform, and the relaxed samples where the strain is neither uniform nor biaxial.

This fact can be understood by the following considerations. In samples with defects strain is not uniform but, except for the volumes around the defect cores, has a modulation on a mesoscopic scale (i.e., on a length scale larger than a lattice cell size, but smaller than the sample dimensions). Thus it is possible to divide the bulk of the layer in small volumes where the strain tensor can be considered constant and Eq. (4) can applied to obtain the corresponding bond deformation. In other words, Eq. (4) transforms the strain distribution in a corresponding bond lengths distribution. On the basis of this consideration, it is then obvious that the mean values of the two distributions are still related by Eq. (4) even when the strain is not constant over the measured volume. This is what the agreement with the experimental data shown in Fig. 6 actually means.

This argument is not, however, valid for the small volume elements containing the core of the defects, where high distortions are not accounted for by the first order approximation leading to Eq. (4). Nevertheless, their statistical weight on the overall volume of the sample is expected to give rise only to a weak tail in the distribution of bond lengths and thus to be completely negligible in the determination both of the average bond length and of the mean strain.

Summarizing the above considerations we can say that the strain relaxation process not only induces a shift of the bond length distribution but also a broadening due to the strain variation and asymmetry. However, this broadening is convoluted with the contributions due to thermal vibrations and alloying disorder. The measured Debye–Waller parameters include all these contributions; their values are reported in Table I and appear to be constant at a mean value of $(3.1\pm0.4)10^{-3}$ Å^2 for all the samples. In other words, from XAFS it was not possible to observe any broadening due to strain effects. This fact can be easily explained considering that on the basis of Eq. (5), the strain asymmetry for the most asymmetric sample (**B**) leads to a bond length distribution difference between ($\delta r_{+}^{\mathrm{st}}$ and $\delta r_{-}^{\mathrm{st}}$) at most equal to $\pm10^{-2}$ Å.

This value corresponds to an increase of the Debye–Waller factor of 10^{-4} Å^2, four times smaller than the statistical error of the XAFS measurements. Furthermore, the strain nonuniformity measured by HRXRD is at most equal to 0.8×10^{-3}. This number brings to an increase of the Debye-Waller factor smaller than 10^{-4} Å^2. Therefore, the thermal and static disorder are the most important terms determining the broadening of the bond length distributions. This is true obviously for pseudomorphic samples but our results show that it holds also for our relaxed samples that we have deliberately chosen to be largely affected by extended defects and structured surface morphology.

V. CONCLUSIONS

In this work we have measured by XAFS the mean Ga-As bond length in InGaAs epitaxial films undergoing an increasing amount of strain relaxation by the formation of extended defects. As is well known the bond length in a bulk alloy is determined by the composition of the alloy. In a previous article we have demonstrated that a deformation of the bulk bond lengths occur when the alloy film is epitaxially strained. Studying pseudomorphic samples we showed that this deformation varies linearly with the amount of strain. In

the present work we have demonstrated that when various extended defects are present in the samples the bond length deformation is also a linear function of the mean strain. We have also shown that the proportionality constant between the bond length deformation and the mean strain is the same for pseudomorphic and for defective samples and that it can be calculated on the basis of an analytical model which simply applies the mean macroscopic deformations to a local level. The effect on the bond length distribution of asymmetric strain relaxation (typical of this kind of tensile films) was discussed by means of an equation relating the parallel strains in the two ⟨110⟩ directions to a bimodal distribution of the bond lengths. The broadening of the bond length distribution due to the strain nonuniformity and asymmetry was estimated and compared to the broadening introduced by thermal and alloying disorder, demonstrating that it does not affect the value of the XAFS Debye–Waller factor in a detectable way.

[1] E. Bernard and A. Zunger, Phys. Rev. B **34**, 5992 (1986).
[2] A. M. Saitta, S. de Gironcoli, and S. Baroni, Phys. Rev. Lett. **80**, 4939 (1998).
[3] L. V. Kulik, D. A. Hits, M. W. Dashiell, and J. Kolodzei, Appl. Phys. Lett. **72**, 1972 (1998).
[4] L. Nordheim, Ann. Phys. (Leipzig) **9**, 641 (1931).
[5] L. Nordheim, Ann. Phys. (Leipzig) **9**, 606 (1931).
[6] J. C. Mikkelsen and J. B. Boyce, Phys. Rev. B **28**, 7130 (1983).
[7] A. Balzarotti, A. Kisiel, N. Motta, M. Zimnal-Starnawska, M. T. Czycyk, and M. Podgorny, Phys. Rev. B **30**, 2295 (1984).
[8] J. L. Martins and A. Zunger, Phys. Rev. B **30**, 6217 (1984).
[9] Y. Cai and M. F. Thorpe, Phys. Rev. B **46**, 15872 (1992).
[10] J. C. Woicik, J. G. Pellegrino, B. Steiner, K. E. Miyano, S. B. Bompadre, L. B. Sorensen, T.-L. Lee, and S. Khalid, Phys. Rev. Lett. **79**, 5026 (1997).
[11] F. Romanato, D. De Salvador, M. Berti, A. Drigo, M. Natali, M. Tormen, G. Rossetto, S. Pascarelli, F. Boscherini, C. Lamberti, and S. Mobilio, Phys. Rev. B **57**, 14619 (1998).
[12] J. C. Woicik, Phys. Rev. B **57**, 6266 (1998).
[13] Y. Kuwahara, H. Oyanagi, R. Shioda, Y. Takeda, H. Yamaguchi, and M. Aono, Jpn. J. Appl. Phys., Part 1 **33**, 5631 (1994).
[14] M. Tabuchi, T. Kumamoto, and Y. Takeda, J. Appl. Phys. **77**, 143 (1994).
[15] M. Servidori, F. Cembali, R. Fabbri, and A. Zani, J. Appl. Crystallogr. **25**, 46 (1992).
[16] S. Pascarelli, F. Boscherini, F. D'Acapito, J. Hrdy, C. Meneghini, and S. Mobilio, J. Synchrotron Radiat. **3**, 147 (1996).
[17] A. Filipponi, A. Di Cicco, and C. R. Natoli, Phys. Rev. B **52**, 15122 (1995); A. Filipponi and A. Di Cicco, Phys. Rev. B **52**, 15135 (1995).
[18] B. R. Bennett and J. A. del Alamo, J. Electron. Mater. **20**, 1075 (1991).
[19] A. V. Drigo, M. Natali, M. Berti, D. De Salvador, G. Rossetto, G. Torzo, G. Carta, L. Lazzarini, and G. C. Salviati, ''Strain relaxation under compressive or tensile stress,'' Conference Proceedings of Lattice Mismatched and Heterovalent Thin Film Epitaxy, Barga, Italy, 13–18 September 1998.